Molecular Cell
Article

Highly Complementary Target RNAs Promote Release of Guide RNAs from Human Argonaute2

Nabanita De,[1] Lisa Young,[2] Pick-Wei Lau,[1] Nicole-Claudia Meisner,[3] David V. Morrissey,[2] and Ian J. MacRae[1,*]
[1]Department of Integrative Structural and Computational Biology, The Scripps Research Institute, La Jolla, CA 92121, USA
[2]Novartis Institutes for Biomedical Research, 250 Massachusetts Avevnue, Cambridge, MA 02139, USA
[3]Novartis Institutes for Biomedical Research, Novartis Campus, 4002 Basel, Switzerland
*Correspondence: macrae@scripps.edu
http://dx.doi.org/10.1016/j.molcel.2013.04.001

SUMMARY

Argonaute proteins use small RNAs to guide the silencing of complementary target RNAs in many eukaryotes. Although small RNA biogenesis pathways are well studied, mechanisms for removal of guide RNAs from Argonaute are poorly understood. Here we show that the Argonaute2 (Ago2) guide RNA complex is extremely stable, with a half-life on the order of days. However, highly complementary target RNAs destabilize the complex and significantly accelerate release of the guide RNA from Ago2. This "unloading" activity can be enhanced by mismatches between the target and the guide 5′ end and attenuated by mismatches to the guide 3′ end. The introduction of 3′ mismatches leads to more potent silencing of abundant mRNAs in mammalian cells. These findings help to explain why the 3′ ends of mammalian microRNAs (miRNAs) rarely match their targets, suggest a mechanism for sequence-specific small RNA turnover, and offer insights for controlling small RNAs in mammalian cells.

INTRODUCTION

Small RNAs (21–23 nt in length), including microRNAs (miRNAs), small interfering RNAs (siRNAs), and Piwi-interacting RNAs (piRNAs), are regulatory molecules that function in many facets of eukaryotic biology, including developmental timing (Lee et al., 1993), viral defense (Hamilton and Baulcombe, 1999), and protection against selfish genetic elements (Vagin et al., 2006). Small RNAs exert their regulatory functions from within ribonucleoprotein complexes generically termed RISCs (RNA-induced silencing complexes) (Hammond et al., 2000). The core subunit of RISC is a small RNA bound to a member of the Argonaute family of proteins (Rivas et al., 2005). Argonaute uses the small RNA as a guide to identify complementary target transcripts for silencing through a variety of mechanisms, including direct cleavage (Elbashir et al., 2001; Liu et al., 2004), translational repression (Olsen and Ambros, 1999), mRNA decay (Lim et al., 2005), DNA methylation (Mette et al., 2000; Watanabe et al., 2011), and formation of heterochromatin (Volpe et al., 2002).

Most miRNAs are transcribed as long primary-miRNAs by RNA polymerase II (Lee et al., 2004). Pre-miRNA hairpins are excised from primary transcripts by the nuclear ribonuclease III (RNase III) enzyme Drosha (Lee et al., 2003). The resulting pre-miRNAs are shuttled by exportin-5 to the cytoplasm (Bohnsack et al., 2004; Lund et al., 2004; Yi et al., 2003), where they are cleaved into miRNA duplexes by the cytoplasmic RNase III, Dicer (Grishok et al., 2001; Hutvágner et al., 2001; Ketting et al., 2001). Dicer also produces siRNA duplexes from long dsRNAs (Bernstein et al., 2001), which are derived from transcription of endogenous loci or during viral replication (for review, see Kim et al., 2009). The resulting RNA duplexes, which are ~22 nt long and contain a 5′ phosphate and two-base 3′ overhang on each end (Bernstein et al., 2001; Elbashir et al., 2001), are loaded into Argonaute (Hammond et al., 2001; Matranga et al., 2005; Rand et al., 2005) with the aid of chaperone proteins (Iki et al., 2010; Iwasaki et al., 2010; Johnston et al., 2010; Miyoshi et al., 2010; Specchia et al., 2010; Tahbaz et al., 2004). A 5′ phosphate on the guide RNA is a requirement for loading (Lima et al., 2009; Nykänen et al., 2001; Schwarz et al., 2003; Ma et al., 2005; Parker et al., 2005) and is important for fidelity in cleavage site selection on target RNAs (Rivas et al., 2005). The orientation of the small RNA duplex in Argonaute determines which strand is to be retained as the guide for gene silencing—the RNA strand with its 5′ and 3′ ends bound to the MID and PAZ domains of Argonaute, respectively, is retained as the guide (Ma et al., 2004, 2005; Parker et al., 2005; Schirle and MacRae, 2012). The other RNA strand, termed the passenger, is removed and degraded by the nuclease C3PO (Liu et al., 2009; Ye et al., 2011). piRNAs are likely loaded into Piwi proteins (a separate clade of the Argonaute family) as long single-stranded RNAs (Houwing et al., 2007; Vagin et al., 2006), which are subsequently trimmed down to ~22 nt (Kawaoka et al., 2011).

While the mechanisms of small RNA biogenesis have been extensively studied, much less is known about how small RNAs are turned over and degraded. In general, mature miRNAs are believed to be remarkably stable, with lifetimes on the order of days or even weeks in living cells and tissues (Baccarini et al., 2011; Hutvágner et al., 2001; van Rooij et al., 2007). However, a growing number of studies indicate that in some cellular contexts specific mature miRNAs are considerably less stable than others (Bail et al., 2010; Cazalla et al., 2010; Hwang et al., 2007; Krol et al., 2010a; Kuchen et al., 2010; Rissland et al., 2011). For example, some members of the extended miR-16 family are constitutively unstable in mouse 3T3 cells, allowing dynamic transcriptional control of the family during the cell cycle (Rissland et al., 2011). Similarly, rapid miRNA turnover in mouse retinas allows levels of miR-204 and miR-211 to change in response to

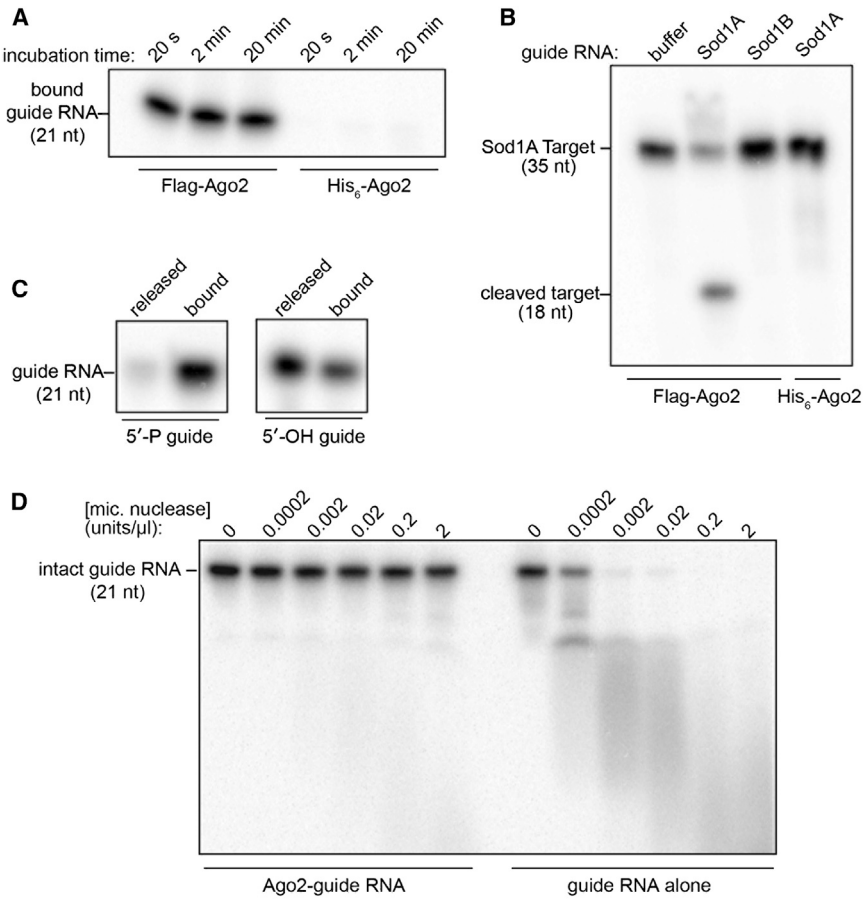

Figure 1. Single-Stranded siRNAs Load into Ago2

(A) Denaturing gel of the single-stranded 5′ ^{32}P-labeled siRNA retained on immobilized Ago2 after incubating at 37°C for indicated times.

(B) Denaturing gel separating full-length and cleaved target RNAs incubated with Ago2 after loading with the corresponding single-stranded guide siRNA.

(C) Denaturing gel showing 5′ P (left panel) or 5′ OH (right panel) guide RNAs bound to and released from immobilized Ago2 upon addition of excess unlabeled guide RNA.

(D) Denaturing gel of equivalent amounts of 5′ ^{32}P-labeled guide RNA, bound to Ago2 or in free solution, after incubation with micrococcal nuclease.

light (Krol et al., 2010b). During mouse T cell differentiation, while most miRNA levels remain constant, miR-150 is rapidly lost as naive T cells differentiate into Th1 and Th2 lymphocytes (Monticelli et al., 2005). And both *Herpesvirus saimiri* and mouse cytomegalovirus have mechanisms for specifically reducing cellular levels of miR-27 during infection (Cazalla et al., 2010; Libri et al., 2012; Marcinowski et al., 2012). Similarly, heterologous expression of highly complementary target RNAs has been shown to promote the loss of mature miRNAs in flies and mammals with an accompanied accumulation of 3′ trimmed and tailed miRNA species (Ameres et al., 2010; Xie et al., 2012).

A variety of ribonucleases have been implicated in small RNA degradation (Rüegger and Großhans, 2012). In cultured human cells, exosome subunit RRP41, a member of the RNase PH family; the cytoplasmic exoribonuclease XRN1 (Bail et al., 2010); and polynucleotide phosphorylase (Das et al., 2010) have all been implicated in degradation of mature miRNAs. In *Caenorhabditis elegans*, XRN2 degrades the miRNA *let-7* (Chatterjee and Grosshans, 2009). In *Arabidopsis thaliana*, five small RNA degrading nucleases (SDNs), distant relatives of RNase T, contribute to miRNA decay (Ramachandran and Chen, 2008), while in the green alga *Chlamydomonas reinhardtii*, the peripheral exosome subunit RRP6, a relative of RNase D, is required for degradation of 3′ uridylated miRNAs (Ibrahim et al., 2010). It is not yet known if these nucleases can degrade small RNAs that are bound within Argonaute; however, *C. elegans* XRN2 degrades *let-7* molecules upon release from Argonaute (Chatterjee and Grosshans, 2009). Therefore, understanding miRNA decay and the factors contributing to small RNA stability requires a detailed understanding of the interactions between Argonaute and its loaded guide RNA.

Here we show that human Argonaute2 (Ago2) has an extremely high affinity for single-stranded guide RNAs, with an off rate on the order of days in vitro. This high-affinity interaction provides substantial protection from nuclease activity in vitro. We also show that, surprisingly, binding of a complementary target RNA can accelerate the dissociation of guide RNAs from Ago2 by several orders of magnitude. Destabilization of the Ago2-guide complex is sensitive to the identity of the guide RNA 5′ nucleotide and attenuated by mismatches between the 3′ end of the guide and target RNAs. We also provide evidence that target RNAs likely affect the Ago2-guide RNA interaction in a similar manner in living cells. These results provide insights into the interactions between Argonaute, guide RNAs, and target RNAs, which are integral to understanding control of small RNA stability in vivo.

RESULTS

Guide RNA-Ago2 Dissociation Is Extremely Slow

Human RISC activity can be reconstituted in vitro by adding a single-stranded guide RNA to purified recombinant Ago2 (Liu et al., 2004; Rivas et al., 2005). To further characterize the interaction between Ago2 and guide RNA, we immobilized FLAG-tagged Ago2 on anti-FLAG agarose and incubated with a single-stranded ^{32}P-labled 21 nt guide RNA (see Table S1 and Table S2 online). The immobilized Ago2 bound the guide RNA rapidly—occupancy of the guide RNA on the resin reached a maximum in less than 20 s (Figure 1A). Binding was Ago2 dependent because anti-FLAG resin treated with cell extract containing His$_6$-tagged Ago2 did not appreciably bind the RNA

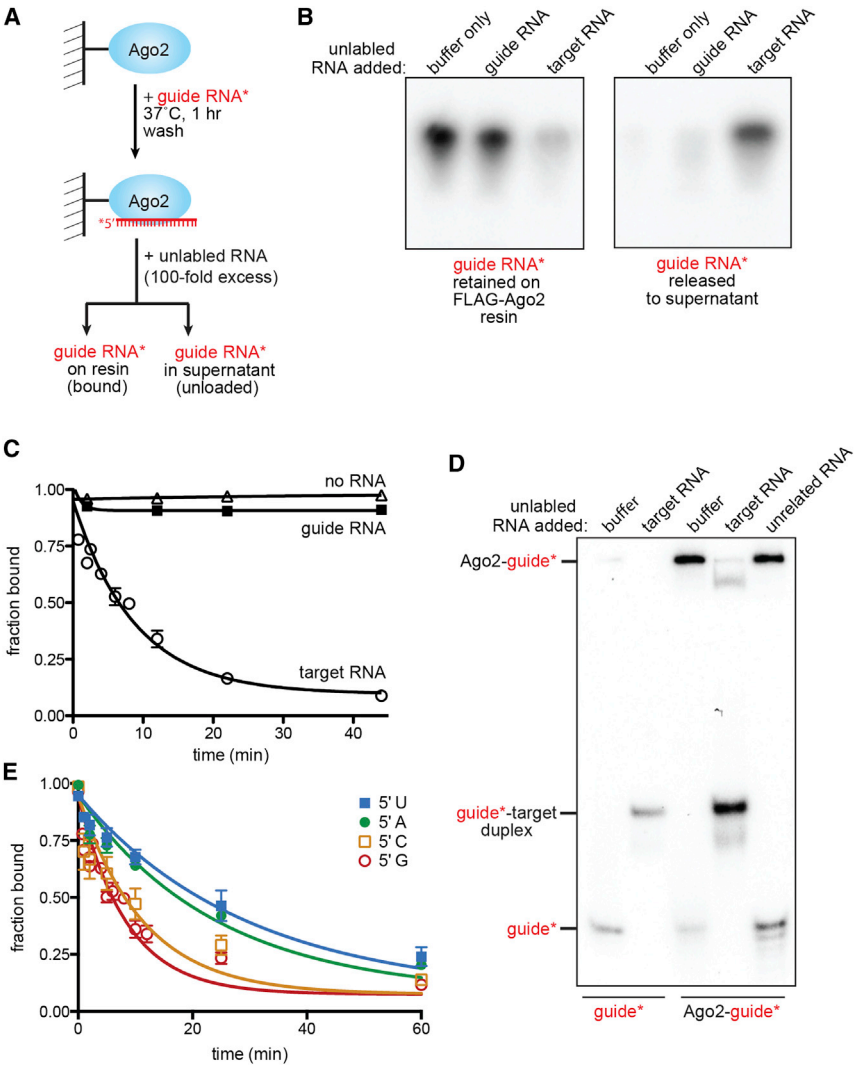

Figure 2. Target RNAs Promote Release of Guide RNAs from Ago2

(A) Schematic of unloading assay: FLAG-Ago2 was immobilized on anti-FLAG agarose, loaded with ^{32}P-labeled guide RNA, and washed extensively before the addition of excess unlabeled RNA.

(B) Denaturing gel of labeled guide RNA bound to and released from Ago2 upon addition of buffer only, unlabeled guide RNA, or complement RNA.

(C) Time course of unloading in the presence of buffer, guide, or complement RNA.

(D) Native gel of Ago2-guide RNA (5′ ^{32}P-labeled) incubated in the presence of buffer alone, an excess of complementary target RNA, or an unrelated, noncomplementary RNA.

(E) Time course of unloading guide RNAs bearing either a 5′ U, A, C, or G. Plotted data are represented as mean ± SEM from at least three independent experiments.

(Figure 1A). After incubation with the single-stranded guide RNA, the immobilized Ago2 catalyzed cleavage, or "slicing," of the corresponding target RNA, indicating that the single-stranded guide RNA was loaded into Ago2 in a catalytically competent conformation (Figure 1B). Based on the pre-steady-state burst of slicing activity from Ago2 associated with a known amount of guide RNA, we estimate that 90% of the guide RNA molecules are competent for slicing (Figure S1).

We next measured the rate of guide RNA-Ago2 dissociation by incubating immobilized, ^{32}P-labeled guide-loaded Ago2 with a 100-fold excess of unlabeled guide RNA. Upon addition of the unlabeled RNA, about 10% of the labeled RNA rapidly dissociated from the resin, suggesting that this fraction was weakly associated with Ago2. The bulk of the labeled guide RNA, however, remained tightly bound (Figure 1C). In fact, even after extended incubation times (>18 hr at 37°C), we observed no decrease in the amount of bound guide RNA. In contrast, guide RNAs that did not have a 5′ phosphate dissociated from the resin (Figure 1C). We conclude that the Ago2-guide RNA complex is extremely stable and that a 5′ phosphate on the small RNA is required for long-lived association with Ago2 (Figure 1C).

The slow dissociation rate of guide RNAs from Ago2 suggested that binding to the protein might provide substantial protection of the RNA from nucleases and degradation. To test this hypothesis, we incubated equivalent amounts of a 5′ end ^{32}P-labeled 21 nt RNA either bound to Ago2 or in free solution with micrococcal nuclease for 15 min at room temperature (Figure 1D). This experiment revealed that binding to Ago2 indeed stabilizes small RNAs in the presence of nuclease. Assuming the rate of degradation is proportional to the nuclease concentration used, we estimate that binding to Ago2 enhances small RNA stability >100,000-fold. This observation is consistent with structural studies of Argonaute that observed guide RNAs bound to a central cleft, which is narrow and deep enough to occlude most nucleases (Elkayam et al., 2012; Nakanishi et al., 2012; Schirle and MacRae, 2012).

Target RNAs Promote Release of Guide RNAs from Ago2

Heterologous expression of miRNA targets has been shown to alter levels of the corresponding mature miRNAs in mammalian cells (Ameres et al., 2010; Baccarini et al., 2011; Kuchen et al., 2010) and in adult mice (Xie et al., 2012). We therefore examined the effect of target RNAs on the interaction between Ago2 and its guide RNA. Immobilized and loaded Ago2 was incubated with a 100-fold excess of unlabeled target RNA that had perfect base-pairing complementarity to the bound guide RNA (Figure 2A). Surprisingly, incubation with the complementary RNA induced dissociation of the guide strand (Figure 2B). A time course study revealed that guide dissociation, or unloading, in the presence of saturating complementary RNA follows

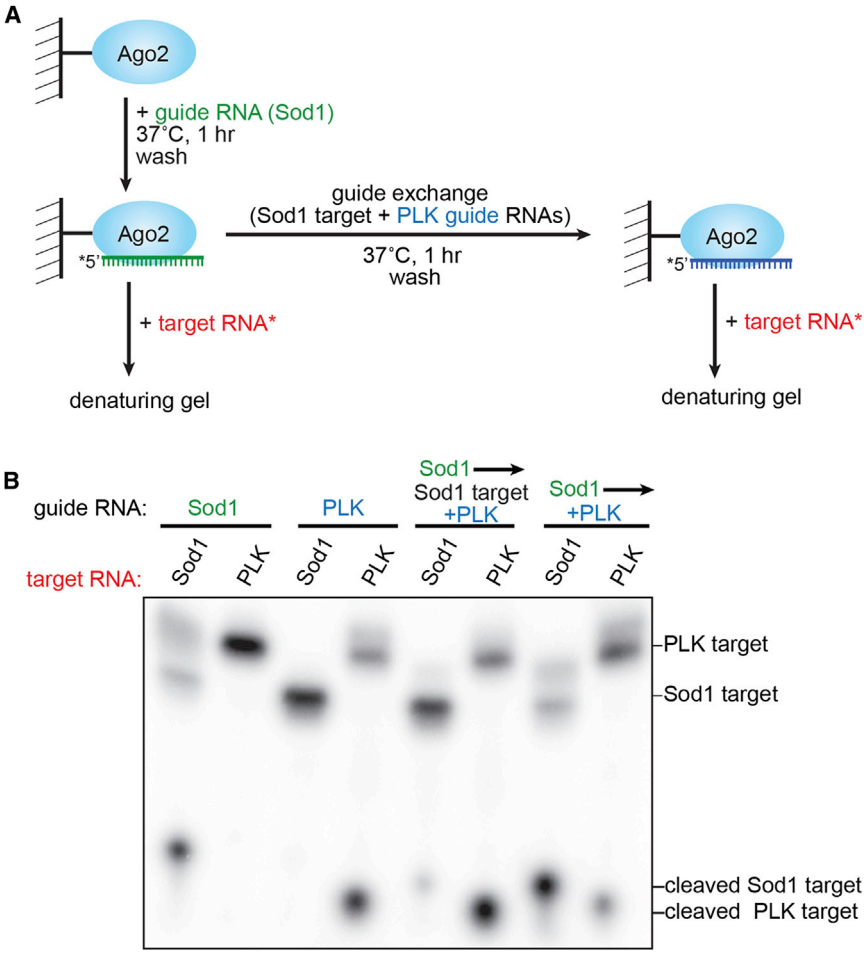

Figure 3. Ago2 Can Be Reprogrammed via Unloading

(A) Schematic (B) and denaturing gel of slicing reactions using immobilized Ago2 before and after reprogramming via unloading. Slicing reactions using Ago2 loaded directly with either Sod1 or PLK guide RNAs served as positive controls. The guide and target RNAs used are labeled, with an arrow indicating an exchange reaction.

first-order kinetics with a half-life of about 6 min (k_{off} = 0.002 s^{-1}) (Figure 2C). Therefore, the target RNA accelerated the dissociation rate of the guide RNA from Ago2 >500-fold. Several other pairs of guide/complement RNA sequences showed similar rate enhancements (see below). A dilution series revealed that although our standard reactions were performed at high target RNA concentrations (3 μM), a similar loss of guide RNA from Ago2 occurs using lower concentrations (3 nM) (Figure S2). We also observed guide unloading from Ago2 in free solution, demonstrating that unloading is not an artifact of immobilizing Ago2 (Figure 2D).

Guide Unloading Is Sensitive to the Identity of the Guide 5′ Nucleotide

Human miRNAs have a 5′ nucleotide bias toward either adenine (A) or uridine (U) (Hu et al., 2009; Kawamata et al., 2011; Lau et al., 2001). This bias has been explained by the finding that the MID domain of Ago2, which binds the 5′ nucleotide of guide RNAs, has about a 20-fold higher affinity for A and U than for guanine (G) and cytosine (C) (Frank et al., 2010). Differences in 5′ nucleotide affinity are proposed to influence guide-strand selection during RISC loading (Ameres et al., 2011; Mi et al., 2008; Seitz et al., 2011). To examine how guide 5′ nucleotide identity contributes to unloading, we compared the rates of unloading of guide RNAs containing either a 5′ U, A, C, or G in the presence of saturating target RNA (Figure 2E). As above, the guide RNA with a 5′ G dissociated from Ago2 in the presence of target with a half-life of about 6 min. The guide with a 5′ C behaved similarly, with a half-life of about 7.5 min. In contrast, guides that contained a 5′ A or U dissociated with half-lives of 17 and 20 min, respectively. Therefore, the presence of a 5′ U or A is insufficient to block unloading but does slow the process. In this case, the presence of a 5′ U reduced the rate of unloading about 3.5-fold compared to a 5′ G.

Guide Unloading Allows Reprogramming of Ago2 In Vitro

Removal of a guide RNA via unloading should leave the RNA-binding cleft of Ago2 vacant, which in principle could allow the "reprograming" of Ago2 with a new guide. We explored this idea by unloading a guide RNA from Ago2 in the presence of an unrelated guide RNA (Figure 3A). Immobilized Ago2 was first loaded with an unlabeled guide RNA (Sod1) and then washed to remove unbound material. The resulting Ago2 displayed slicing activity of the Sod1 target (Figure 3B). We next performed a guide RNA exchange reaction by adding a mixture of the Sod1 target RNA (which had a 5′ hydroxyl) and an unrelated PLK guide RNA (bearing a 5′ phosphate) to the resin. A reaction that did not include the Sod1 target was used to control for unloading-independent changes. After 1 hr the RNA mixtures were removed and the resins were tested for slicing activity. Slicing of the Sod1 target was reduced after the exchange reaction. The loss of Sod1 slicing activity was accompanied by the acquisition of robust slicing activity of PLK target RNA. In contrast, the sample that was not treated with Sod1 target retained Sod1 slicing activity and displayed only weak activity against the PLK target. These results suggest that upon unloading of the Sod1 guide RNA, Ago2 was loaded with PLK guide RNA. The reprogrammed Ago2 had slicing activity comparable to the activity of the singly loaded enzyme, suggesting that loading/unloading is a reversible and nondestructive process. We conclude that the

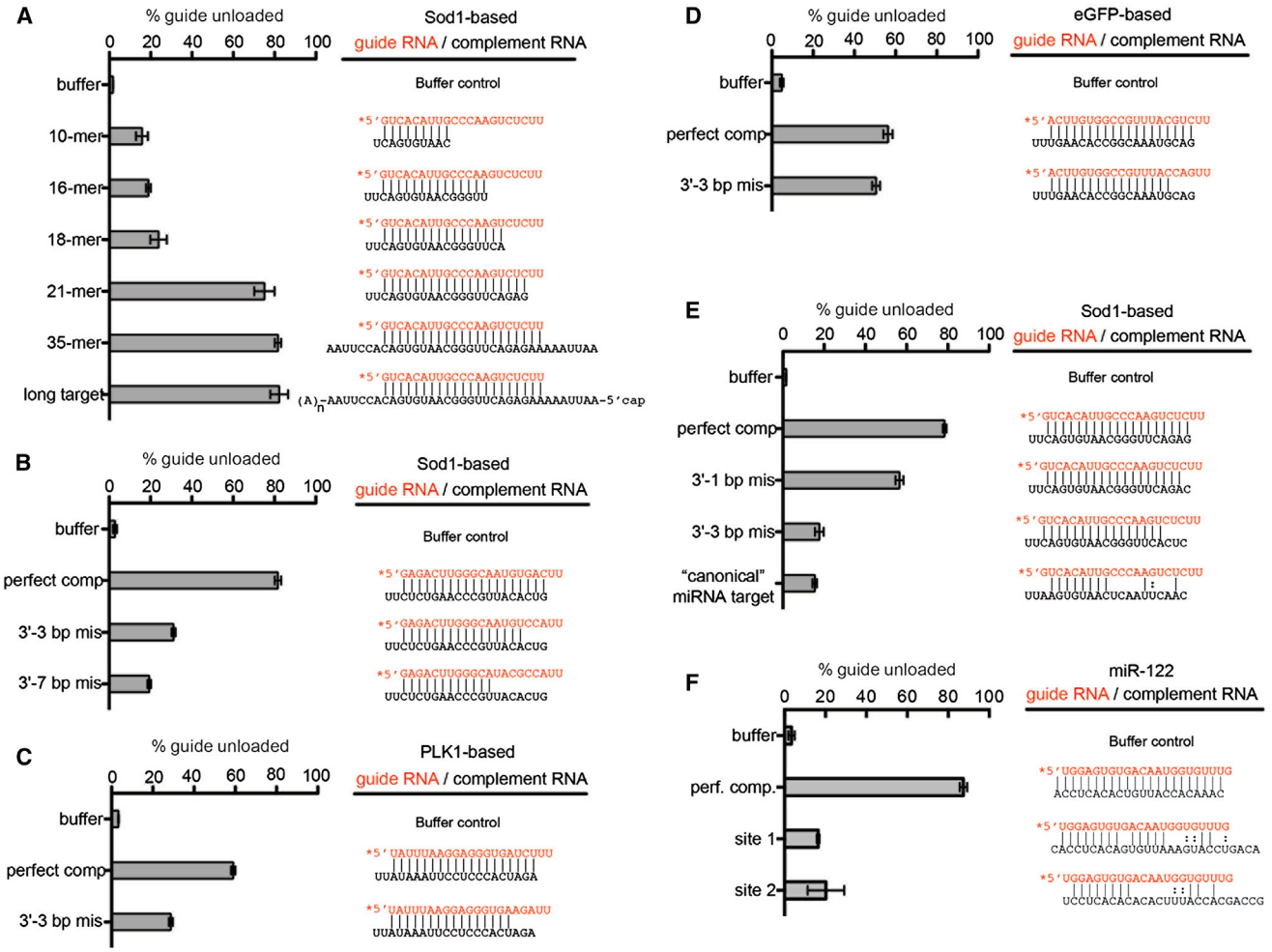

Figure 4. Complementarity to the 3′ End of the Guide Facilitates Unloading

(A) Percent of guide RNA unloaded from Ago2 by complement RNAs after a 20 min incubation. Schematics of paired guide and complement RNAs are shown in the right panel.

(B–D) Percent guide unloaded by complement RNAs bearing mismatches to the 3′ ends of Ago2-bound guide RNAs. Nucleotide sequences tested are variations of siRNAs against superoxide dismutase-1 (Sod1) (B), polo-like kinase-1 (PLK1) (C), and enhanced green fluorescent protein (eGFP) (D).

(E) Guide unloading by a canonical miRNA target—perfect match, one mismatch, and three mismatch complements are included for comparison.

(F) Inefficient unloading of miR122 guide by natural target sites. Data are represented as mean ± SEM from at least three independent experiments.

unloading reaction allows the recycling and reprogramming of Ago2 proteins in vitro.

Mismatches to the Guide 3′ End Inhibit Unloading

The crystal structure of Ago2 suggests that the first eight nucleotides (from the 5′ end) of the guide RNA are the most tightly associated with Ago2 (Schirle and MacRae, 2012). However, we found that a small RNA complementary to nucleotides 1–9 of the guide was unable to promote unloading during a 20 min incubation (Figure 4A). In fact, even an RNA complementary to bases 1–16 was a poor unloader. In contrast, target RNAs that paired either with bases 1–19 or with the entire guide RNA catalyzed unloading efficiently (Figure 4A). These data suggest that either a full-length complement is required for unloading or that base-pairing to the 3′ end of the guide is critical. Including an m^7G cap and poly(A) tail on the target RNA does not inhibit unloading (Figure 4A).

To examine the 3′ base-pairing requirements of unloading, we monitored the effects of 21 nt target RNAs with mismatches to the 3′ end of several different guide RNAs (Figures 4B–4F). In general, mismatches to the 3′ end of the guide RNAs reduced the amount of guide RNA unloaded from Ago2 during a 20 min incubation. In one case, even a single mismatch in the 3′ end was sufficient to noticeably reduce the amount unloaded (Figure 4E). These 3′ mismatches are most likely not inhibitory to unloading due to a reduced affinity for the RNA target, because increasing target concentrations by 10-fold gave similar results (data not shown). A small RNA designed to mimic a canonical miRNA target (Bartel, 2009) was a poor unloader in our assay (Figure 4E), as were two validated target sites for miR-122 from

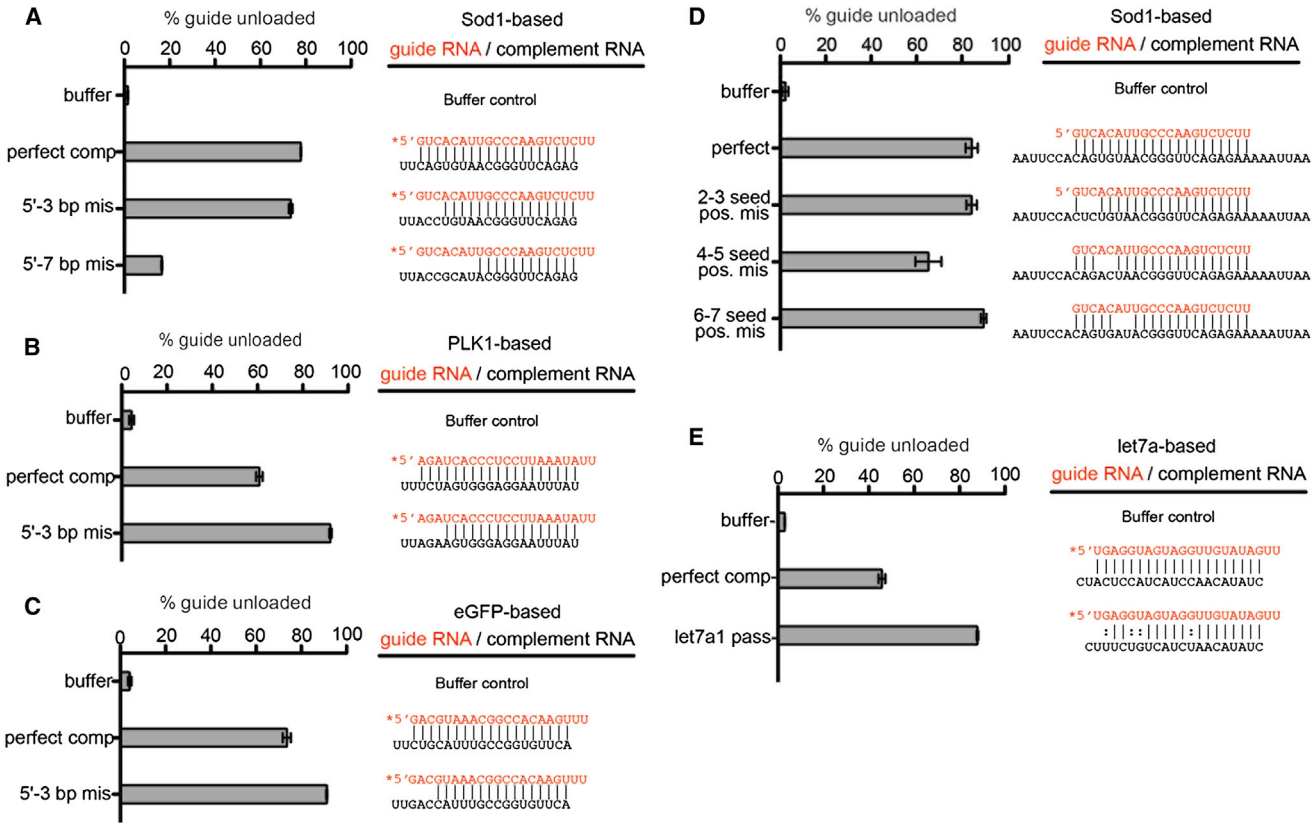

Figure 5. Mismatches to the Guide 5′ End Can Facilitate Unloading

(A–C) Percent of guide RNA unloaded from Ago2 by complement RNAs bearing mismatches to the 5′ ends of Ago2-bound guide RNAs. Schematics of paired guide and complement RNAs are shown in the right panel.

(D) Unloading by targets with mismatches to the guide seed region.

(E) Unloading of let-7a by its perfect complement or miR passenger strand. Data are represented as mean ± SEM from at least three independent experiments.

the 3′UTR of the cationic amino acid transporter-1 mRNA (Chang et al., 2004) (Figure 4F).

5′ Mismatches Can Facilitate Unloading

We next examined how mismatches between the 5′ end of the guide and the target affect unloading. A variety of guide RNAs were loaded into immobilized Ago2 as single strands and then incubated with 21 nt targets with various degrees of complementarity for 20 min (Figures 5A–5C). In contrast to 3′ mismatches, mismatches to the 5′ end of the guide tended not to inhibit unloading. These experiments revealed that, although the seed region (nucleotides 2–7) contributes significantly to the affinity for target RNAs (Haley and Zamore, 2004; Wee et al., 2012), base-pairing to the three terminal nucleotides on the 5′ end of the guide is not required for unloading when the target RNA is saturating (5 μM). However, unlike 3′ mismatches, 5′ mismatches reduced the rate of unloading relative to a perfect complement at lower target concentrations (<3 nM) (data not shown). We also found that unloading is not strongly inhibited by dinucleotide mismatches in the seed sequence (Figure 5D). We note that with two of the three sequences examined, mismatches to guide nucleotides 1–3 led to more unloading during the 20 min incubation than the corresponding perfect complements (Figures 5B and 5C). Similarly, the natural passenger strand of let-7a (let-7a1*) unloaded more let-7a than the perfect let-7a complement during a 20 min incubation (90% versus 42% unloaded, p = 0.002, paired t test) (Figure 5E).

Target RNAs Promote Release of Guide RNAs from Human RISC In Vitro

Argonaute is the core subunit of RISC and the only known protein to stably associate with mature small RNAs (Rivas et al., 2005; Tomari et al., 2004). We therefore examined the ability of target RNAs to accelerate dissociation of guide RNAs from human RISC. First, we monitored the association of an siRNA with RISC in the presence and absence of target RNA in cell extracts (Figure 6A). Cytoplasmic extracts from HEK293 cells stably expressing FLAG-Ago2 were prepared and incubated with a ^{32}P 5′ end-labeled siRNA duplex for 1 hr using RISC assembly protocols (Ameres et al., 2007). After RISC assembly, m^{7}G-capped, polyadenylated, fully complementary target RNA was added, and the extract was incubated at 37°C for another hour. Immunoprecipitation (IP) of Ago2 revealed that introducing high concentrations of target RNA into the extract for 1 hr reduced the amount of guide RNA associated with RISC by more than 70% (Figure 6B). Next, we observed release of the guide RNA

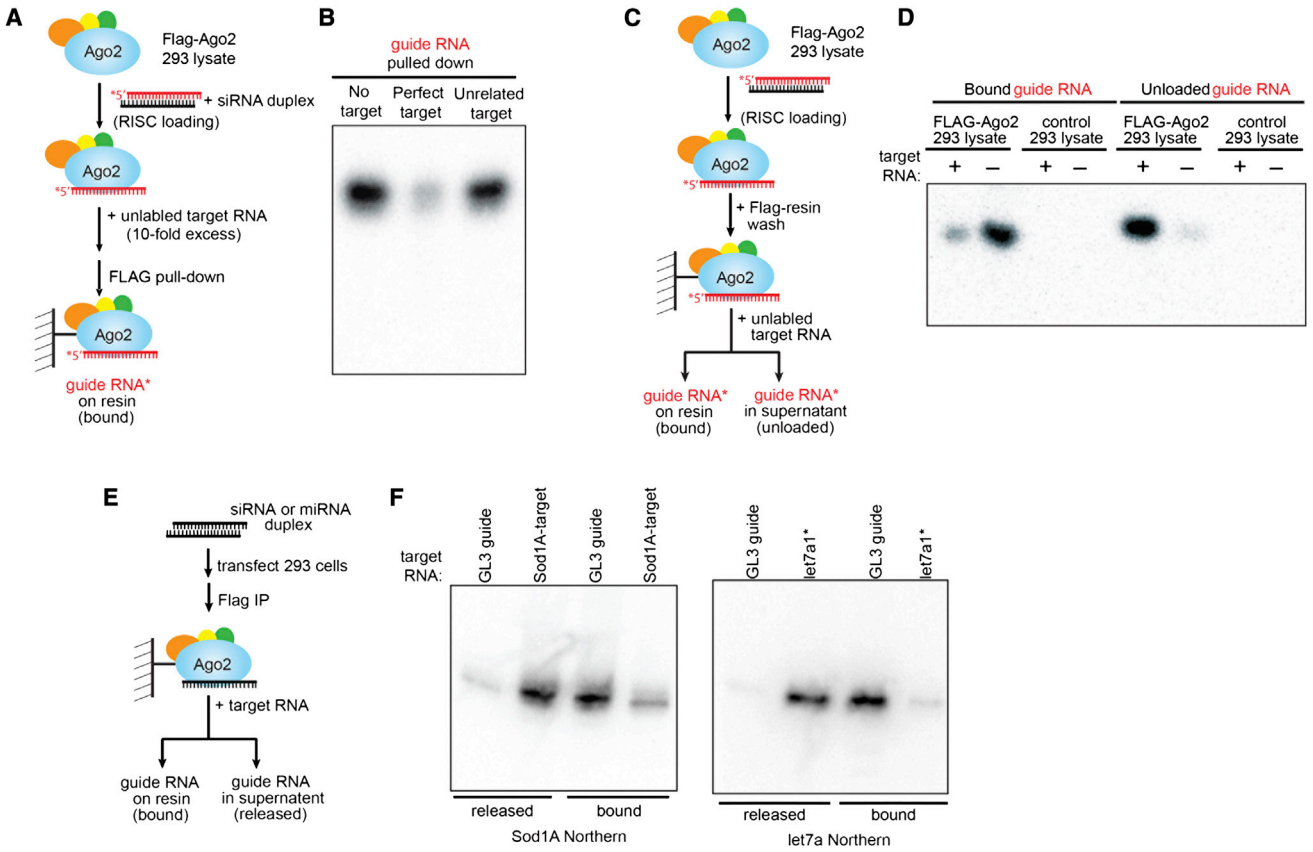

Figure 6. Guide RNAs Are Unloaded from RISC by Target RNAs

(A and B) (A) Schematic and (B) denaturing gel of RISC-unloading experiment in 293 cell extract.

(C and D) Unloading of immobilized RISC. Mock 293 extract (from cells not expressing FLAG-Ago2) was included as a negative control.

(E and F) (E) Schematic and (F) northern blot of Sod1 (left panel) and let-7a1 (right panel) duplex transfected into FLAG-Ago2 293 cells released from RISC upon treatment with complementary RNAs or unrelated RNA (GL3 guide).

from RISC by immobilizing the complex before adding the target RNA. Bound and released fractions were separated after 60 min (Figures 6C and 6D). In a time course experiment, we found that unloading in cell extract is similar to that observed in a simple buffer system, except that in cell extract the unloaded guide RNAs were less stable and degraded (Figure S3). Finally, we examined unloading of guide RNAs from RISC that had been assembled in living cells (Figure 6E). FLAG-Ago2 was immunopurified from HEK293 cells that had been transfected with siRNA and miRNA (let-7a1) duplexes. Addition of the corresponding target RNA, but not an unrelated control RNA (GL3), promoted release of siRNA or miRNA guide from immobilized RISC (Figure 6F). We conclude that target RNAs facilitate the release of guide RNAs from human RISC in vitro.

Target RNAs that Promote Unloading Reduce Ago2-siRNA Levels in Living Cells

The introduction of a target RNA into mammalian cells or animals can lead to reductions in the levels of the miRNAs bearing high complementarity to the target (Ameres et al., 2010; Baccarini et al., 2011; Kuchen et al., 2010; Xie et al., 2012). Target-induced miRNA depletion was proposed to be the result of an increased rate of miRNA degradation that is triggered by RISC:target interactions (Ameres et al., 2010; Baccarini et al., 2011). Considering the extraordinary protection that is provided to guide RNAs associated with Ago2, we wondered if target-induced degradation in living cells operates through a guide RNA release mechanism similar to that observed during unloading in extracts. We therefore asked if target-induced miRNA depletion involves a loss of guide RNA from Ago2 and, if so, if Ago2 depletion is sensitive to the same factors as in vitro unloading—namely, identity of the guide 5′ nucleotide as well as mismatches between the target and the ends of the guide RNA.

We generated a series of *Renilla* luciferase expression constructs wherein three tandem target sites were placed in the 3′UTR, and different reporters had differing degrees of complementarity to our guide siRNA (Figure 7A). Target plasmids were transfected into HEK293 cells with siRNA duplexes containing either a 5′ G or a 5′ U on the guide strand. After 45 hr, cells were lysed, and the amount of siRNA associated with Ago2 was measured by FLAG-IP and northern blotting. A let-7a1 duplex, which is normally expressed at low levels in our cell line (Figure S4A), was cotransfected to normalize for differences

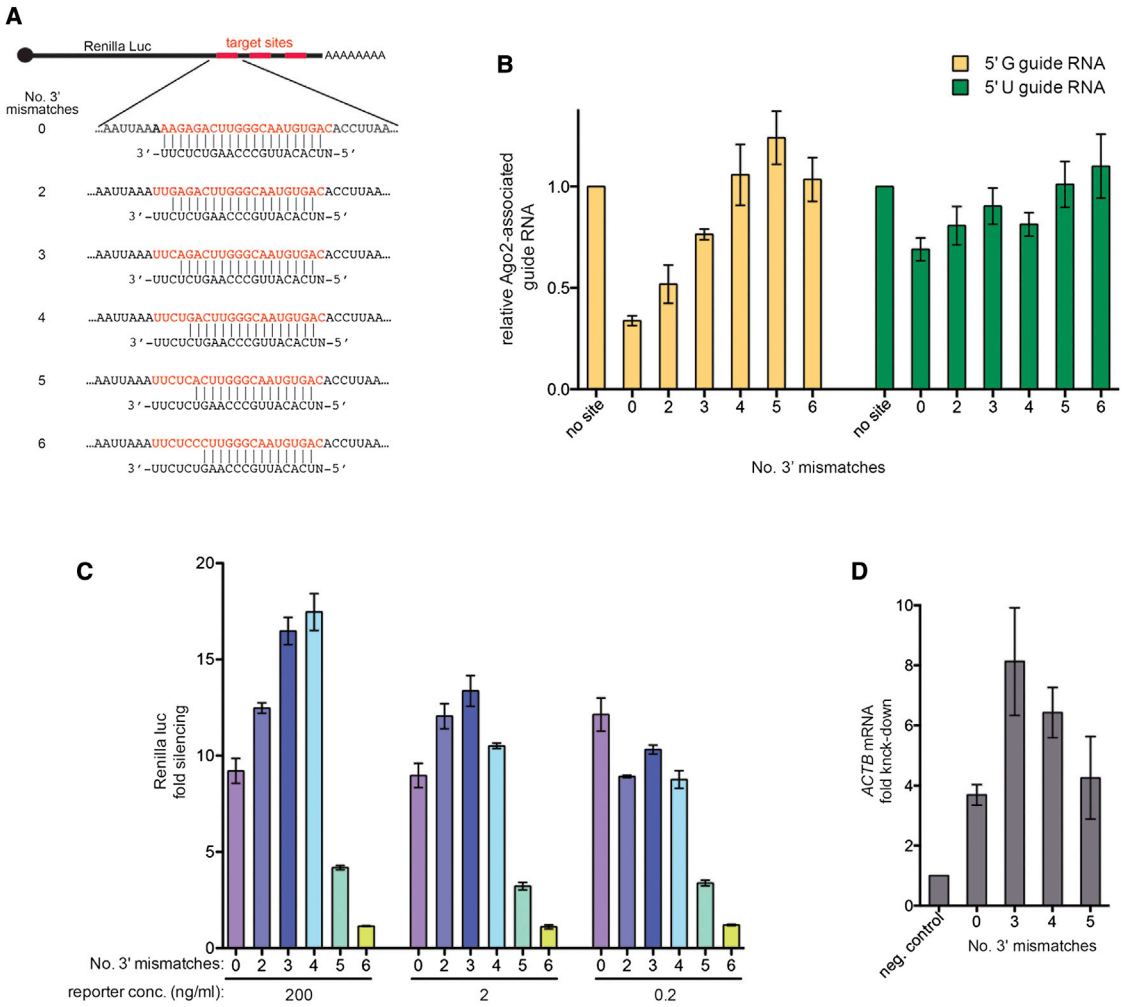

Figure 7. 3′ Mismatches Enhance Silencing of Abundant Transcripts

(A) Schematic of target constructs paired to guide siRNA.

(B) Quantification of guide siRNAs (5′ G and 5′ U, yellow and green, respectively) associated with Ago2 after cotransfection with perfect and 3′ mismatch target constructs. Data were normalized to the amount of siRNA associated with Ago2 when transfected with a reporter with no siRNA target sites. Data are represented as mean ± SEM from three independent experiments.

(C) Fold silencing (luc – siRNA/luc + siRNA) of *Renilla* reporters with mismatches to the 3′ end of the guide siRNA. Concentrations of reporter DNA in transfections are indicated.

(D) Fold knockdown of *ACTB* mRNA by siRNAs with 3′ mismatches to a common site in the message. Mean ± SEM from three biological replicates is shown.

in transfection and IP efficiency. The relative amounts of both 5′ G and 5′ U siRNAs associated with Ago2 were reduced in cells overexpressing the perfect target RNA compared to the nontarget site control (Figure 7B). Similar results were obtained from HEK293 cells using an anti-Ago2 monoclonal antibody for IP (Figures S4B and S4C). Adding a 2′-o-methyl group to the 3′-terminal ribose of the guide RNA did not protect the guide from target-induced depletion from Ago2 (Figure S4C). Expression of the perfect target reduced Ago2 association of the 5′ G siRNA significantly more than the 5′ U siRNA (66% versus 31% reduction, p = 0.017, paired t test). Increasing the number of mismatches between the target and the 3′ end of the guide RNAs reduced the amount of siRNA depleted from Ago2 (Figure 7B). We also found that targets bearing 5′ mismatches to the guide RNA can reduce the amount of guide RNA associated with Ago2 in cells (Figures S4D and S4E). However, 5′ mismatches did not significantly enhance the effect, possibly because, unlike our in vitro unloading reactions, cellular concentrations of target RNAs may not be high enough to overcome the reduced affinity of Ago2 for targets containing mismatches to the guide seed region (Wee et al., 2012). We conclude that overexpression of target RNAs in HEK293 cells reduces the amount of corresponding guide RNAs associated with Ago2. Moreover, like in vitro unloading, target-induced guide RNA depletion is sensitive to the identity of the guide 5′ nucleotide and mismatches to the guide RNA 3′ end.

3′ Mismatches Can Enhance Silencing of Abundant Transcripts

Target cleavage via the slicing reaction necessarily requires siRNAs to be bound by Ago2 (Rivas et al., 2005). We therefore hypothesized that the protective effect that 3′ mismatches have on the siRNA-Ago2 association might give rise to more potent gene silencing than siRNAs with perfect complementarity. To test this idea, various amounts of our *Renilla* target plasmids (Figure 7A) were transfected with and without the targeting siRNA into HEK293 cells. A firefly cotransfection control was included, as well as a luciferase-free plasmid which was used to maintain a fixed total DNA concentration in all transfections. Expression of *Renilla* constructs bearing perfect target sites was reduced 9-fold by the siRNA (Figure 7C). While, as expected, a large number of 3′ mismatches (five or more) reduced silencing by the siRNA, a few mismatches increased the ability of the siRNA to silence the luciferase reporter: the introduction of two 3′ mismatches significantly increased repression ($p = 0.034$, paired t test), and three mismatches resulted in even greater silencing ($p = 0.024$, paired t test). Indeed, four mismatches reduced expression of the reporter by more than 17-fold. Adding a 2′-o-methyl group to the 3′-terminal ribose of the guide RNA did not reduce the effect of 3′ mismatches (data not shown), and two unrelated siRNA/target sequences showed a similar trend (Figures S4F–S4I). Importantly, reducing reporter levels abrogated the enhanced silencing observed with 3′ mismatches such that, at the lowest reporter concentration tested, all mismatches reduced silencing compared to the perfect target sites (Figure 7C, right panel). We conclude that 3′ mismatches can enhance gene silencing in mammalian cells and observe a correlation between the optimal number of mismatches and the abundance of the target transcript.

The reporter experiments suggested that including 3′ mismatches in siRNAs might be beneficial for improving the knockdown of highly expressed endogenous transcripts. We explored this hypothesis by transfecting HEK293 cells with siRNAs bearing various 3′ mismatches to β-actin (*ACTB*) mRNA and measuring mRNA levels 48 hr after transfection (Figure 7D). While the perfectly complementary siRNA was only able to knock down message levels 3.6-fold, siRNAs with three and four 3′ mismatches knocked down *ACTB* mRNA to a greater extent (7.4-fold and 6.2-fold, respectively; $p = 0.072$ and $p = 0.039$, unpaired t test). Enhanced silencing by the siRNAs with 3′ mismatches was not due to more efficient small RNA processing or loading, because the same siRNAs were less potent than the perfect *ACTB* siRNA when targeting luciferase reporters with sites perfectly complementary to each (Figure S4J).

DISCUSSION

Here we show that target RNAs can destabilize the interaction between human Ago2 and guide RNA in vitro and provide evidence that the effect likely occurs in living cells as well. These findings are consistent with the observation that Ago2 has a lower affinity for double-stranded than single-stranded RNA (Lima et al., 2009). This discovery demonstrates that loading of a guide RNA into Ago2 is a reversible process. Importantly, both long target RNAs and short (21 nt) complementary RNAs can promote release of a guide RNA. This leads us to hypothesize that, in vivo, Ago2 may bind and release small RNA duplexes multiple times before eventually committing to a guide RNA by removal of the passenger strand—thereby switching from a low-affinity interaction with the small RNA duplex to a high-affinity interaction with the single-stranded guide. Consistent with this idea, the natural passenger strand of let-7a is a potent unloader of let-7a, revealing that the let-7a1 miRNA duplex can dissociate from Ago2 rapidly (Figure 5E). Surprisingly, in several cases mismatches to the guide 5′ end enhanced the rate of unloading compared to perfectly paired complement RNAs. This observation raises the possibility that reduced pairing to the guide 5′ end may effectively lower the energy barrier for moving small RNA duplexes into and out of Ago2. Dynamic loading and unloading could provide a sampling mechanism by which Ago2 identifies and preferentially retains guide RNAs bearing 5′ U or A nucleotides. This model also suggests that Ago2 could function as a sensor of siRNA and miRNA duplex asymmetry (Khvorova et al., 2003; Schwarz et al., 2003).

In the absence of targets, guide RNAs dissociate from Ago2 at a very slow rate, with a half-life on the order of days, or possibly weeks. This observation is reminiscent of the suggestion that the loading of an siRNA into RISC is an irreversible process (Martinez et al., 2002). The slow off rate of guide RNAs, taken with the protection from nuclease degradation offered by Argonaute, may explain why mature miRNAs often have half-lives on the order of days or even weeks in living cells (Baccarini et al., 2011; Gantier et al., 2011; van Rooij et al., 2007). Indeed, although we find that highly complementary target RNAs decrease the affinity of Ago2 for its guide, 3′ mismatches significantly attenuate this phenomenon. Mismatches between the 3′ end of a guide RNA and its target are prevalent in mammalian miRNA target sites (Bartel, 2009), suggesting that the majority of identified miRNA targets do not destabilize the interaction between Ago2 and the cognate miRNA. Taken together, these results provide a plausible explanation for the high stability of small RNAs that has been observed in vivo and in cell lysate (Hutvágner et al., 2001; van Rooij et al., 2007).

On the other hand, in some biological contexts miRNA stability is regulated and specific miRNAs are targeted for accelerated decay (Avraham et al., 2010; Bail et al., 2010; Cazalla et al., 2010; Das et al., 2010; Hwang et al., 2007; Krol et al., 2010a; Kuchen et al., 2010; Rissland et al., 2011; Sethi and Lukiw, 2009). While the mechanism(s) by which miRNAs are targeted for degradation is not yet well understood, a few miRNA-specific models have begun to emerge (Rüegger and Großhans, 2012). Due to the protective effects of binding to Argonaute, we predict that all miRNA degradation pathways have to contend with the high-affinity interaction between Argonaute and its bound miRNA. Our results reveal that binding to a target with extensive complementarity, particularly to the miRNA 3′ end, dramatically reduces this barrier. We therefore hypothesize that some miRNA decay mechanisms may capitalize on this effect. Indeed, the *Herpesvirus saimiri* U RNA-1 (HSUR-1) has been shown to base pair with miR-27 and specifically promote its downregulation, with pairing between HSUR-1 and the 3′ end of miR-27 a requirement of miR-27 degradation (Cazalla et al., 2010). Similarly, murine cytomegalovirus generates a transcript termed

m169 that, like HSUR-1, bears extensive complementarity to the 3′ end and seed region of miR-27 and promotes a significant reduction in miR-27 levels during viral infection (Libri et al., 2012; Marcinowski et al., 2012). However, a synthetic HSUR-1 fragment was a poor unloader in vitro, suggesting that additional factors may be involved in cellular degradation of miR-27 (data not shown). Additionally, the overexpression of a complementary target RNA in mammalian cells has been shown to promote miRNA decay with an accompanying increase in the levels of 3′ trimmed and tailed miRNA species (Ameres et al., 2010; Baccarini et al., 2011). Like unloading, trimming and tailing require pairing between the miRNA 3′ end and target RNA (Ameres et al., 2010; Baccarini et al., 2011), suggesting that these processes may also utilize the reduced interactions between Argonaute and guide RNA that we observe upon target binding.

Our results also have implications for design of anti-miRs (chemical antagonists of miRNAs) and synthetic siRNAs. Anti-miRs can act as competitive inhibitors of miRNA function, i.e., by sequestering a miRNA, but not changing its cellular concentration (Davis et al., 2009; Elmén et al., 2008; Torres et al., 2011), or by promoting miRNA degradation (Esau et al., 2006; Krützfeldt et al., 2005; Torres et al., 2011). We suggest that, in principle, an anti-miR that promotes unloading and degradation of a released miRNA, without degradation of the anti-miR itself, could act catalytically and be significantly more potent than anti-miRs using a stoichiometric sequestration mechanism. For siRNA optimization, we find that including 3′ mismatches between the antisense strand and its target stabilizes the interaction between Ago2 and siRNA both in vitro and in living cells. 3′ mismatches also facilitate release of cleaved target RNAs and thereby can increase the rate of turnover by RISC (Ameres et al., 2007; Haley and Zamore, 2004). Therefore, in principle, 3′ mismatches should give rise to more potent gene silencing. In practice, we find that 3′ mismatches can enhance knockdown significantly, but the effect is strongest when silencing highly expressed target mRNAs and appears to be lost when targeting less abundant transcripts (Figure 7C). The combined results reveal that a detailed structural and mechanistic dissection of the dynamic interplay between Ago2, guide, target, and product RNAs is likely to significantly advance ongoing efforts to harness RNA silencing processes for therapeutic purposes.

EXPERIMENTAL PROCEDURES

Ago2 Preparation, Loading, and Unloading

FLAG-tagged human Ago2 was expressed in Sf9 cells using a baculovirus system and immunopurified from cell lysates using anti-FLAG agarose. Immobilized Ago2 was loaded by incubating with ^{32}P-labeled single-stranded guide RNA. Unbound material was removed by washing the resin. Guide RNAs were unloaded by incubation with an excess (1.5–100 μM) of unlabeled target RNA. The unloaded fraction was isolated by brief centrifugation and careful removal of the supernatant solution. All reactions were carried out at 37°C. Alternatively, loaded Ago2 in free solution was obtained by eluting the protein-RNA complex using a FLAG peptide. RNA samples were analyzed by denaturing polyacrylamide gel electrophoresis and phosphorimaging.

RISC Loading and Unloading

Lysates from HEK293 cells were prepared as described (Ameres et al., 2007). Plasmids and RNAs were transfected into cells using Lipofectamine 2000. Luciferase activity was measured using the Dual-Luciferase Reporter Assay System (Promega). Additional experimental details are included in the Supplemental Information.

SUPPLEMENTAL INFORMATION

Supplemental Information includes four figures, two tables, Supplemental Experimental Procedures, and Supplemental References and can be found with this article at http://dx.doi.org/10.1016/j.molcel.2013.04.001.

ACKNOWLEDGMENTS

We thank P. Zamore for critically reading the manuscript and for thoughtful suggestions, and N. Schirle, J. Sheu-Gruttadauria, and O. Rissland for many important and insightful conversations, ilo-a. P.-W.L. was a predoctoral fellow of the American Heart Association. This work was supported by NIH grant R01 GM086701 to I.J.M.

Received: November 9, 2012
Revised: February 27, 2013
Accepted: March 28, 2013
Published: May 9, 2013

REFERENCES

Ameres, S.L., Martinez, J., and Schroeder, R. (2007). Molecular basis for target RNA recognition and cleavage by human RISC. Cell *130*, 101–112.

Ameres, S.L., Horwich, M.D., Hung, J.H., Xu, J., Ghildiyal, M., Weng, Z., and Zamore, P.D. (2010). Target RNA-directed trimming and tailing of small silencing RNAs. Science *328*, 1534–1539.

Ameres, S.L., Hung, J.H., Xu, J., Weng, Z., and Zamore, P.D. (2011). Target RNA-directed tailing and trimming purifies the sorting of endo-siRNAs between the two Drosophila Argonaute proteins. RNA *17*, 54–63.

Avraham, R., Sas-Chen, A., Manor, O., Steinfeld, I., Shalgi, R., Tarcic, G., Bossel, N., Zeisel, A., Amit, I., Zwang, Y., et al. (2010). EGF decreases the abundance of microRNAs that restrain oncogenic transcription factors. Sci. Signal. *3*, ra43. http://dx.doi.org/10.1126/scisignal.2000876.

Baccarini, A., Chauhan, H., Gardner, T.J., Jayaprakash, A.D., Sachidanandam, R., and Brown, B.D. (2011). Kinetic analysis reveals the fate of a microRNA following target regulation in mammalian cells. Curr. Biol. *21*, 369–376.

Bail, S., Swerdel, M., Liu, H., Jiao, X., Goff, L.A., Hart, R.P., and Kiledjian, M. (2010). Differential regulation of microRNA stability. RNA *16*, 1032–1039.

Bartel, D.P. (2009). MicroRNAs: target recognition and regulatory functions. Cell *136*, 215–233.

Bernstein, E., Caudy, A.A., Hammond, S.M., and Hannon, G.J. (2001). Role for a bidentate ribonuclease in the initiation step of RNA interference. Nature *409*, 363–366.

Bohnsack, M.T., Czaplinski, K., and Gorlich, D. (2004). Exportin 5 is a RanGTP-dependent dsRNA-binding protein that mediates nuclear export of pre-miRNAs. RNA *10*, 185–191.

Cazalla, D., Yario, T., and Steitz, J.A. (2010). Down-regulation of a host microRNA by a Herpesvirus saimiri noncoding RNA. Science *328*, 1563–1566.

Chang, J., Nicolas, E., Marks, D., Sander, C., Lerro, A., Buendia, M.A., Xu, C., Mason, W.S., Moloshok, T., Bort, R., et al. (2004). miR-122, a mammalian liver-specific microRNA, is processed from hcr mRNA and may downregulate the high affinity cationic amino acid transporter CAT-1. RNA Biol. *1*, 106–113.

Chatterjee, S., and Grosshans, H. (2009). Active turnover modulates mature microRNA activity in Caenorhabditis elegans. Nature *461*, 546–549.

Das, S.K., Sokhi, U.K., Bhutia, S.K., Azab, B., Su, Z.Z., Sarkar, D., and Fisher, P.B. (2010). Human polynucleotide phosphorylase selectively and preferentially degrades microRNA-221 in human melanoma cells. Proc. Natl. Acad. Sci. USA *107*, 11948–11953.

Davis, S., Propp, S., Freier, S.M., Jones, L.E., Serra, M.J., Kinberger, G., Bhat, B., Swayze, E.E., Bennett, C.F., and Esau, C. (2009). Potent inhibition of microRNA in vivo without degradation. Nucleic Acids Res. *37*, 70–77.

Elbashir, S.M., Lendeckel, W., and Tuschl, T. (2001). RNA interference is mediated by 21- and 22-nucleotide RNAs. Genes Dev. *15*, 188–200.

Elkayam, E., Kuhn, C.D., Tocilj, A., Haase, A.D., Greene, E.M., Hannon, G.J., and Joshua-Tor, L. (2012). The structure of human argonaute-2 in complex with miR-20a. Cell *150*, 100–110.

Elmén, J., Lindow, M., Schütz, S., Lawrence, M., Petri, A., Obad, S., Lindholm, M., Hedtjärn, M., Hansen, H.F., Berger, U., et al. (2008). LNA-mediated microRNA silencing in non-human primates. Nature *452*, 896–899.

Esau, C., Davis, S., Murray, S.F., Yu, X.X., Pandey, S.K., Pear, M., Watts, L., Booten, S.L., Graham, M., McKay, R., et al. (2006). miR-122 regulation of lipid metabolism revealed by in vivo antisense targeting. Cell Metab. *3*, 87–98.

Frank, F., Sonenberg, N., and Nagar, B. (2010). Structural basis for 5′-nucleotide base-specific recognition of guide RNA by human AGO2. Nature *465*, 818–822.

Gantier, M.P., McCoy, C.E., Rusinova, I., Saulep, D., Wang, D., Xu, D., Irving, A.T., Behlke, M.A., Hertzog, P.J., Mackay, F., and Williams, B.R. (2011). Analysis of microRNA turnover in mammalian cells following Dicer1 ablation. Nucleic Acids Res. *39*, 5692–5703.

Grishok, A., Pasquinelli, A.E., Conte, D., Li, N., Parrish, S., Ha, I., Baillie, D.L., Fire, A., Ruvkun, G., and Mello, C.C. (2001). Genes and mechanisms related to RNA interference regulate expression of the small temporal RNAs that control *C. elegans* developmental timing. Cell *106*, 23–34.

Haley, B., and Zamore, P.D. (2004). Kinetic analysis of the RNAi enzyme complex. Nat. Struct. Mol. Biol. *11*, 599–606.

Hamilton, A.J., and Baulcombe, D.C. (1999). A species of small antisense RNA in posttranscriptional gene silencing in plants. Science *286*, 950–952.

Hammond, S.M., Bernstein, E., Beach, D., and Hannon, G.J. (2000). An RNA-directed nuclease mediates post-transcriptional gene silencing in Drosophila cells. Nature *404*, 293–296.

Hammond, S.M., Boettcher, S., Caudy, A.A., Kobayashi, R., and Hannon, G.J. (2001). Argonaute2, a link between genetic and biochemical analyses of RNAi. Science *293*, 1146–1150.

Houwing, S., Kamminga, L.M., Berezikov, E., Cronembold, D., Girard, A., van den Elst, H., Filippov, D.V., Blaser, H., Raz, E., Moens, C.B., et al. (2007). A role for Piwi and piRNAs in germ cell maintenance and transposon silencing in Zebrafish. Cell *129*, 69–82.

Hu, H.Y., Yan, Z., Xu, Y., Hu, H., Menzel, C., Zhou, Y.H., Chen, W., and Khaitovich, P. (2009). Sequence features associated with microRNA strand selection in humans and flies. BMC Genomics *10*, 413.

Hutvágner, G., McLachlan, J., Pasquinelli, A.E., Bálint, E., Tuschl, T., and Zamore, P.D. (2001). A cellular function for the RNA-interference enzyme Dicer in the maturation of the let-7 small temporal RNA. Science *293*, 834–838.

Hwang, H.W., Wentzel, E.A., and Mendell, J.T. (2007). A hexanucleotide element directs microRNA nuclear import. Science *315*, 97–100.

Ibrahim, F., Rymarquis, L.A., Kim, E.J., Becker, J., Balassa, E., Green, P.J., and Cerutti, H. (2010). Uridylation of mature miRNAs and siRNAs by the MUT68 nucleotidyltransferase promotes their degradation in Chlamydomonas. Proc. Natl. Acad. Sci. USA *107*, 3906–3911.

Iki, T., Yoshikawa, M., Nishikiori, M., Jaudal, M.C., Matsumoto-Yokoyama, E., Mitsuhara, I., Meshi, T., and Ishikawa, M. (2010). In vitro assembly of plant RNA-induced silencing complexes facilitated by molecular chaperone HSP90. Mol. Cell *39*, 282–291.

Iwasaki, S., Kobayashi, M., Yoda, M., Sakaguchi, Y., Katsuma, S., Suzuki, T., and Tomari, Y. (2010). Hsc70/Hsp90 chaperone machinery mediates ATP-dependent RISC loading of small RNA duplexes. Mol. Cell *39*, 292–299.

Johnston, M., Geoffroy, M.C., Sobala, A., Hay, R., and Hutvagner, G. (2010). HSP90 protein stabilizes unloaded argonaute complexes and microscopic P-bodies in human cells. Mol. Biol. Cell *21*, 1462–1469.

Kawamata, T., Yoda, M., and Tomari, Y. (2011). Multilayer checkpoints for microRNA authenticity during RISC assembly. EMBO Rep. *12*, 944–949.

Kawaoka, S., Izumi, N., Katsuma, S., and Tomari, Y. (2011). 3′ end formation of PIWI-interacting RNAs in vitro. Mol. Cell *43*, 1015–1022.

Ketting, R.F., Fischer, S.E., Bernstein, E., Sijen, T., Hannon, G.J., and Plasterk, R.H. (2001). Dicer functions in RNA interference and in synthesis of small RNA involved in developmental timing in C. elegans. Genes Dev. *15*, 2654–2659.

Khvorova, A., Reynolds, A., and Jayasena, S.D. (2003). Functional siRNAs and miRNAs exhibit strand bias. Cell *115*, 209–216.

Kim, V.N., Han, J., and Siomi, M.C. (2009). Biogenesis of small RNAs in animals. Nat. Rev. Mol. Cell Biol. *10*, 126–139.

Krol, J., Busskamp, V., Markiewicz, I., Stadler, M.B., Ribi, S., Richter, J., Duebel, J., Bicker, S., Fehling, H.J., Schübeler, D., et al. (2010a). Characterizing light-regulated retinal microRNAs reveals rapid turnover as a common property of neuronal microRNAs. Cell *141*, 618–631.

Krol, J., Loedige, I., and Filipowicz, W. (2010b). The widespread regulation of microRNA biogenesis, function and decay. Nat. Rev. Genet. *11*, 597–610.

Krützfeldt, J., Rajewsky, N., Braich, R., Rajeev, K.G., Tuschl, T., Manoharan, M., and Stoffel, M. (2005). Silencing of microRNAs in vivo with 'antagomirs'. Nature *438*, 685–689.

Kuchen, S., Resch, W., Yamane, A., Kuo, N., Li, Z., Chakraborty, T., Wei, L., Laurence, A., Yasuda, T., Peng, S., et al. (2010). Regulation of microRNA expression and abundance during lymphopoiesis. Immunity *32*, 828–839.

Lau, N.C., Lim, L.P., Weinstein, E.G., and Bartel, D.P. (2001). An abundant class of tiny RNAs with probable regulatory roles in Caenorhabditis elegans. Science *294*, 858–862.

Lee, R.C., Feinbaum, R.L., and Ambros, V. (1993). The C. elegans heterochronic gene lin-4 encodes small RNAs with antisense complementarity to lin-14. Cell *75*, 843–854.

Lee, Y., Ahn, C., Han, J., Choi, H., Kim, J., Yim, J., Lee, J., Provost, P., Rådmark, O., Kim, S., and Kim, V.N. (2003). The nuclear RNase III Drosha initiates microRNA processing. Nature *425*, 415–419.

Lee, Y., Kim, M., Han, J., Yeom, K.H., Lee, S., Baek, S.H., and Kim, V.N. (2004). MicroRNA genes are transcribed by RNA polymerase II. EMBO J. *23*, 4051–4060.

Libri, V., Helwak, A., Miesen, P., Santhakumar, D., Borger, J.G., Kudla, G., Grey, F., Tollervey, D., and Buck, A.H. (2012). Murine cytomegalovirus encodes a miR-27 inhibitor disguised as a target. Proc. Natl. Acad. Sci. USA *109*, 279–284.

Lim, L.P., Lau, N.C., Garrett-Engele, P., Grimson, A., Schelter, J.M., Castle, J., Bartel, D.P., Linsley, P.S., and Johnson, J.M. (2005). Microarray analysis shows that some microRNAs downregulate large numbers of target mRNAs. Nature *433*, 769–773.

Lima, W.F., Wu, H., Nichols, J.G., Sun, H., Murray, H.M., and Crooke, S.T. (2009). Binding and cleavage specificities of human Argonaute2. J. Biol. Chem. *284*, 26017–26028.

Liu, J., Carmell, M.A., Rivas, F.V., Marsden, C.G., Thomson, J.M., Song, J.J., Hammond, S.M., Joshua-Tor, L., and Hannon, G.J. (2004). Argonaute2 is the catalytic engine of mammalian RNAi. Science *305*, 1437–1441.

Liu, Y., Ye, X., Jiang, F., Liang, C., Chen, D., Peng, J., Kinch, L.N., Grishin, N.V., and Liu, Q. (2009). C3PO, an endoribonuclease that promotes RNAi by facilitating RISC activation. Science *325*, 750–753.

Lund, E., Güttinger, S., Calado, A., Dahlberg, J.E., and Kutay, U. (2004). Nuclear export of microRNA precursors. Science *303*, 95–98.

Ma, J.B., Ye, K., and Patel, D.J. (2004). Structural basis for overhang-specific small interfering RNA recognition by the PAZ domain. Nature *429*, 318–322.

Ma, J.B., Yuan, Y.R., Meister, G., Pei, Y., Tuschl, T., and Patel, D.J. (2005). Structural basis for 5′-end-specific recognition of guide RNA by the A. fulgidus Piwi protein. Nature *434*, 666–670.

Marcinowski, L., Tanguy, M., Krmpotic, A., Rädle, B., Lisnić, V.J., Tuddenham, L., Chane-Woon-Ming, B., Ruzsics, Z., Erhard, F., Benkartek, C., et al. (2012). Degradation of cellular mir-27 by a novel, highly abundant viral transcript is

important for efficient virus replication in vivo. PLoS Pathog. *8*, e1002510. http://dx.doi.org/10.1371/journal.ppat.1002510.

Martinez, J., Patkaniowska, A., Urlaub, H., Lührmann, R., and Tuschl, T. (2002). Single-stranded antisense siRNAs guide target RNA cleavage in RNAi. Cell *110*, 563–574.

Matranga, C., Tomari, Y., Shin, C., Bartel, D.P., and Zamore, P.D. (2005). Passenger-strand cleavage facilitates assembly of siRNA into Ago2-containing RNAi enzyme complexes. Cell *123*, 607–620.

Mette, M.F., Aufsatz, W., van der Winden, J., Matzke, M.A., and Matzke, A.J. (2000). Transcriptional silencing and promoter methylation triggered by double-stranded RNA. EMBO J. *19*, 5194–5201.

Mi, S., Cai, T., Hu, Y., Chen, Y., Hodges, E., Ni, F., Wu, L., Li, S., Zhou, H., Long, C., et al. (2008). Sorting of small RNAs into Arabidopsis argonaute complexes is directed by the 5′ terminal nucleotide. Cell *133*, 116–127.

Miyoshi, T., Takeuchi, A., Siomi, H., and Siomi, M.C. (2010). A direct role for Hsp90 in pre-RISC formation in Drosophila. Nat. Struct. Mol. Biol. *17*, 1024–1026.

Monticelli, S., Ansel, K.M., Xiao, C., Socci, N.D., Krichevsky, A.M., Thai, T.H., Rajewsky, N., Marks, D.S., Sander, C., Rajewsky, K., et al. (2005). MicroRNA profiling of the murine hematopoietic system. Genome Biol. *6*, R71. http://dx.doi.org/10.1186/gb-2005-6-8-r71.

Nakanishi, K., Weinberg, D.E., Bartel, D.P., and Patel, D.J. (2012). Structure of yeast Argonaute with guide RNA. Nature *486*, 368–374.

Nykänen, A., Haley, B., and Zamore, P.D. (2001). ATP requirements and small interfering RNA structure in the RNA interference pathway. Cell *107*, 309–321.

Olsen, P.H., and Ambros, V. (1999). The lin-4 regulatory RNA controls developmental timing in Caenorhabditis elegans by blocking LIN-14 protein synthesis after the initiation of translation. Dev. Biol. *216*, 671–680.

Parker, J.S., Roe, S.M., and Barford, D. (2005). Structural insights into mRNA recognition from a PIWI domain-siRNA guide complex. Nature *434*, 663–666.

Ramachandran, V., and Chen, X. (2008). Degradation of microRNAs by a family of exoribonucleases in Arabidopsis. Science *321*, 1490–1492.

Rand, T.A., Petersen, S., Du, F., and Wang, X. (2005). Argonaute2 cleaves the anti-guide strand of siRNA during RISC activation. Cell *123*, 621–629.

Rissland, O.S., Hong, S.J., and Bartel, D.P. (2011). MicroRNA destabilization enables dynamic regulation of the miR-16 family in response to cell-cycle changes. Mol. Cell *43*, 993–1004.

Rivas, F.V., Tolia, N.H., Song, J.J., Aragon, J.P., Liu, J., Hannon, G.J., and Joshua-Tor, L. (2005). Purified Argonaute2 and an siRNA form recombinant human RISC. Nat. Struct. Mol. Biol. *12*, 340–349.

Rüegger, S., and Großhans, H. (2012). MicroRNA turnover: when, how, and why. Trends Biochem. Sci. *37*, 436–446.

Schirle, N.T., and MacRae, I.J. (2012). The crystal structure of human Argonaute2. Science *336*, 1037–1040.

Schwarz, D.S., Hutvágner, G., Du, T., Xu, Z., Aronin, N., and Zamore, P.D. (2003). Asymmetry in the assembly of the RNAi enzyme complex. Cell *115*, 199–208.

Seitz, H., Tushir, J.S., and Zamore, P.D. (2011). A 5′-uridine amplifies miRNA/miRNA* asymmetry in Drosophila by promoting RNA-induced silencing complex formation. Silence *2*, 4. http://dx.doi.org/10.1186/1758-907X-2-4.

Sethi, P., and Lukiw, W.J. (2009). Micro-RNA abundance and stability in human brain: specific alterations in Alzheimer's disease temporal lobe neocortex. Neurosci. Lett. *459*, 100–104.

Specchia, V., Piacentini, L., Tritto, P., Fanti, L., D'Alessandro, R., Palumbo, G., Pimpinelli, S., and Bozzetti, M.P. (2010). Hsp90 prevents phenotypic variation by suppressing the mutagenic activity of transposons. Nature *463*, 662–665.

Tahbaz, N., Kolb, F.A., Zhang, H., Jaronczyk, K., Filipowicz, W., and Hobman, T.C. (2004). Characterization of the interactions between mammalian PAZ PIWI domain proteins and Dicer. EMBO Rep. *5*, 189–194.

Tomari, Y., Matranga, C., Haley, B., Martinez, N., and Zamore, P.D. (2004). A protein sensor for siRNA asymmetry. Science *306*, 1377–1380.

Torres, A.G., Fabani, M.M., Vigorito, E., and Gait, M.J. (2011). MicroRNA fate upon targeting with anti-miRNA oligonucleotides as revealed by an improved Northern-blot-based method for miRNA detection. RNA *17*, 933–943.

Vagin, V.V., Sigova, A., Li, C., Seitz, H., Gvozdev, V., and Zamore, P.D. (2006). A distinct small RNA pathway silences selfish genetic elements in the germline. Science *313*, 320–324.

van Rooij, E., Sutherland, L.B., Qi, X., Richardson, J.A., Hill, J., and Olson, E.N. (2007). Control of stress-dependent cardiac growth and gene expression by a microRNA. Science *316*, 575–579.

Volpe, T.A., Kidner, C., Hall, I.M., Teng, G., Grewal, S.I., and Martienssen, R.A. (2002). Regulation of heterochromatic silencing and histone H3 lysine-9 methylation by RNAi. Science *297*, 1833–1837.

Watanabe, T., Tomizawa, S., Mitsuya, K., Totoki, Y., Yamamoto, Y., Kuramochi-Miyagawa, S., Iida, N., Hoki, Y., Murphy, P.J., Toyoda, A., et al. (2011). Role for piRNAs and noncoding RNA in de novo DNA methylation of the imprinted mouse Rasgrf1 locus. Science *332*, 848–852.

Wee, L.M., Flores-Jasso, C.F., Salomon, W.E., and Zamore, P.D. (2012). Argonaute divides its RNA guide into domains with distinct functions and RNA-binding properties. Cell *151*, 1055–1067.

Xie, J., Ameres, S.L., Friedline, R., Hung, J.H., Zhang, Y., Xie, Q., Zhong, L., Su, Q., He, R., Li, M., et al. (2012). Long-term, efficient inhibition of microRNA function in mice using rAAV vectors. Nat. Methods *9*, 403–409.

Ye, X., Huang, N., Liu, Y., Paroo, Z., Huerta, C., Li, P., Chen, S., Liu, Q., and Zhang, H. (2011). Structure of C3PO and mechanism of human RISC activation. Nat. Struct. Mol. Biol. *18*, 650–657.

Yi, R., Qin, Y., Macara, I.G., and Cullen, B.R. (2003). Exportin-5 mediates the nuclear export of pre-microRNAs and short hairpin RNAs. Genes Dev. *17*, 3011–3016.